Analysis of Tunable Laser Heterodyne Radiometry: Remote Sensing of Atmospheric Gases

R. K. SEALS JR.*
NASA Langley Research Center, Hampton, Va.

A theoretical analysis of high spectral resolution (<0.01 cm^{-1}) remote sensing of atmospheric gas profiles with a tunable infrared laser heterodyne radiometer at satellite altitudes is presented. Numerical simulations are given for retrievals of H_2O vapor and CH_4 profiles assuming a tunable diode laser as the heterodyne local oscillator. Line-by-line calculations of atmospheric thermal emissions are made in selected frequency intervals and used in sample retrievals of profiles of these gases from 0 to 30 km altitude. The potential of this technique for providing maximum vertical resolution with minimum interference effects is demonstrated. Error analyses using expected radiometer signal-to-noise errors, temperature bias errors, and ground temperature errors indicate that retrieval profiles with less than 20% average error can be obtained.

Introduction

REMOTE sensing of the vertical distribution of atmospheric and pollutant gas concentrations from satellite or space shuttle altitudes has many applications in pollution control, meteorology, and atmospheric physics. In principle, if the atmospheric temperature profile is known, the vertical distribution of a gas can be determined by spectrally scanning the upwelling thermal radiance from an infrared emission band of the gas and applying mathematical inversion techniques to retrieve the distribution profile from the radiance data.[1,2] Vertical resolution is obtained by using the fact that the atmospheric transmittance is a strong function of frequency in spectral regions containing gas absorption-emission bands,[3] with maximum vertical resolution being provided by detection with infinite spectral resolution. High spectral resolution, of the order of 10^{-3} cm^{-1}, is also necessary for measurement of gas concentrations in the upper atmosphere since radiation from this region originates from very near the line centers of Doppler-broadened emission lines.

Remote measurements of atmospheric H_2O vapor content and temperature have been made from Nimbus altitudes using a spectrometer (5 cm^{-1} spectral resolution) to detect the thermal radiance from portions of the 11 to 36 μm region of the spectrum.[4,5] However, limitations on this type of measurement are imposed both by interference from overlapping bands of other gases and by the low spectral resolution. An instrument such as the selective chopper radiometer[6,7] is capable of the high spectral resolution necessary for near maximum altitude resolution and altitude range. However, interference effects still impose a limit on this type of instrument, particularly in the troposphere, since it sums the radiances from narrow portions of many emission lines.

The purpose of this paper is to demonstrate that a high spectral resolution radiometer capable of scanning individual atmospheric emission lines can provide remote sensing of the vertical distribution of atmospheric gases with minimum interference from overlapping gases and near maximum altitude resolution and range. Specific calculations are given for a nadir viewing system operating at satellite altitudes and consisting of a heterodyne radiometer with a tunable diode laser local oscillator. Laser heterodyne radiometry is essentially a passive remote sensing technique since upwelling atmospheric thermal radiances provide the signal. However, an active laser source is involved in the detection scheme. The laser provides a local oscillator (LO) signal which is mixed with the incoming radiance signals at a high-frequency detector to yield signals at difference frequencies of the order of 1 GHz or less. More detailed discussions of heterodyne detection and of some of its applications are available in the literature.[8-12] Use of a narrow linewidth tunable diode laser as the heterodyne LO provides flexibility in the selection of optimum sensing frequencies and allows spectral resolution which is limited only by signal level. In this paper, the capability of this system for measurements of the vertical distributions of atmospheric H_2O vapor and CH_4 between 0 and 30 km altitude is illustrated by numerical retrievals of distribution profiles from simulated radiance data in the 7 to 8 μm spectral region. This portion of the infrared spectrum has considerable overlap between bands of various gases and is used here to demonstrate the strength of the heterodyne radiometer in such regions. The effects of radiance detection errors, distributed temperature errors, temperature bias errors, and ground temperature errors on the gas profile retrievals are illustrated numerically and discussed along with typical radiometer signal-to-noise levels.

Theory

In laser heterodyne radiometry, the thermal radiance N_j in a spectral channel of bandwidth β centered at frequency ν_j is mixed with a laser LO signal at ν_{LO} to provide a signal at the difference frequency $\nu_D = |\nu_j - \nu_{LO}|$. However, the system actually responds to the sum of signals in radiance channels centered at $\nu_{LO} \pm \nu_D$, and the desired signal of the channel at ν_j is summed with the signal of an image channel with respect to ν_{LO}. A tunable LO such as a diode laser allows constructive use of this image channel. This is illustrated in Fig. 1 which shows the variation of atmospheric radiance with frequency and illustrates the two types of spectral tuning available in a tunable laser heterodyne radiometer. The cross-hatched areas indicate the signal channel and its image channel. Case I tuning, used to detect radiances from the wings of emission lines, involves tuning ν_{LO} while keeping ν_D fixed at a value slightly greater than $\beta/2$. The spectral

Presented as Paper 73-703 at the AIAA 6th Fluid and Plasma Dynamics Conference, Palm Springs, Calif., July 16–18, 1973; submitted July 16, 1973; revision received February 12, 1974. The author would like to thank F. Allario for suggesting this work and also P. Brockman for his many helpful comments. Computer programs used in this analysis can be obtained from the author, along with limited documentation.

Index categories: Atmospheric, Space, and Oceanographic Sciences; Lasers.

* Aerospace Technologist, Environmental and Space Sciences Division. Associate Member AIAA.

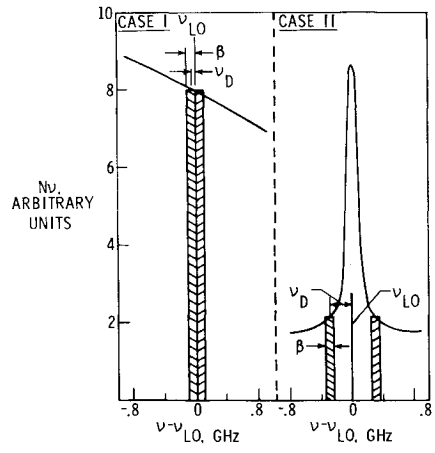

Fig. 1 Atmospheric radiance vs frequency illustrating spectral tuning of a tunable heterodyne radiometer. (Cross-hatched areas denote the signal and image channels.)

resolution in this case is $\simeq 2\beta$. Individual laser modes of available diode lasers can be tuned over ranges of at least 45 GHz (1.5 cm^{-1}) with current tuning or 10 GHz (0.33 cm^{-1}) with magnetic field tuning.[13] Case II tuning, used for channels near atmospheric emission line centers, utilizes the emission line symmetry to ensure that the radiances in the signal channel and its image channel are equal. The LO frequency is fixed while ν_D is tuned over a range limited by detector response to a maximum value of 1 to 2 GHz (0.033 to 0.067 cm^{-1}). In this case the spectral resolution is β. In both cases the tunable LO provides added versatility over a fixed frequency LO and allows a set of sensing channels to be chosen which both optimizes altitude coverage and minimizes interference from other gases. Use of a fixed frequency laser LO with less than an exact coincidence with the sensing channel or emission line of interest would require additional data processing and interpretation to account for the image channel radiance.

Single mode LO powers of the order of 1 to 10 mw are required to provide quantum-limited operation of a heterodyne detector. Such power levels are being approached with diode lasers and appear to be within the capability of existing technology. For an ideal case with quantum-limited operation, unit quantum efficiency, and zero excess noise, the signal-to-noise ratio of a heterodyne radiometer for a radiance channel at ν, and a bandwidth β is given by

$$SNR = (c^2N/2h\nu^3)(t/\beta)^{1/2} \tag{1}$$

where h, c, and t are Planck's constant, the speed of light, and the postdetection integration time, respectively. N is the sum of the radiant powers (per unit emitter area and solid angle) for the signal channel and its image and is given by

$$N = \int_{\nu_{LO}-\nu_D-\beta/2}^{\nu_{LO}-\nu_D+\beta/2} N_\nu\, d\nu + \int_{\nu_{LO}+\nu_D-\beta/2}^{\nu_{LO}+\nu_D+\beta/2} N_\nu\, d\nu \tag{2}$$

where N_ν is the atmospheric radiant power (per unit emitter area, solid angle, and bandwidth) at frequency ν.

For a nonscattering atmosphere in local thermodynamic equilibrium, N_ν at level y_t is given by

$$N_\nu = B_\nu(0)\tau_\nu(0) + \int_0^{y_t} [B_\nu(y)][\partial\tau_\nu(y)/\partial y]\, dy \tag{3}$$

where $y = -\ln(p/p_o)$, $B_\nu(y)$ is Planck's radiation function at ν and level y, $\tau_\nu(y)$ is the transmittance at ν between levels y and y_t, p is the pressure at level y, and the subscripts o and t refer to ground and upper atmosphere limits. Equation (3) applies to a cloudless field of view, and additional terms are necessary for consideration of clouds. The first term in Eq. (3) is the ground contribution for a ground emissivity of unity, and the second term is the integrated contribution from all atmospheric levels. The mass fraction ω_i of the ith absorbing gas, defined as the ratio of the mass density of gas i to that of the atmosphere at level y, is to be determined. For i absorbing gases, ω_i is contained in the transmittance τ_ν given by

$$\tau_\nu(y) = \exp\left(-C\sum_i \int_y^{y_t} k_i(y)\omega_i(y)\, e^{-y}\, dy\right) \tag{4}$$

where k_i is the absorption coefficient of gas i at ν and y and C is a constant. The signal N_j for the jth channel of a heterodyne radiometer is given by

$$N_j = B_j(0)\tau_j(0) + \int_0^{y_t} [B_j(y)][\partial\tau_j(y)/\partial y]\, dy \tag{5}$$

where $B(\nu, y)$ has been replaced by a mean value $B_j(y) = B(\nu_j, y)$ and where[14]

$$\begin{aligned} \tau_j(y) &= (1/\Delta\nu_j)\textstyle\int_{\Delta\nu_j} \tau_\nu(y)\, d\nu \\ \partial\tau_j(y)/\partial y &= (1/\Delta\nu_j)\textstyle\int_{\Delta\nu_j} [\partial\tau_\nu(y)/\partial y]\, d\nu \end{aligned} \tag{6}$$

assuming a symmetrical response function. For Case I channels $\nu_j = \nu_{LO}$, $\Delta\nu_j$ is the frequency range from $\nu_{LO}-\beta$ to $\nu_{LO}+\beta$, and N_j is the total signal received by the radiometer. For Case II channels $\nu_j = \nu_{LO} \pm \nu_D$ is the center of the signal channel, $\Delta\nu_j$ is the frequency range from $\nu_j-\beta/2$ to $\nu_j+\beta/2$, and N_j is half of the total received signal. For this paper β has been taken as 10^8 Hz (0.0033 cm^{-1}).

The altitude range covered by channel j is determined by the weighting function $\partial\tau_j(y)/\partial y$. Retrieval of an altitude profile of ω_i using Eq. (5) requires several sensing channels with each containing information from a limited altitude range. Several methods exist for inverting Eq. (5) to retrieve $\omega_i(y)$ from a set of radiances N_j. In all cases the atmospheric temperature profile must be known. The method used in this work follows the iterative procedure of Smith[1] which has the advantage of providing solutions which are not prespecified to a certain analytical form and do not depend significantly on empirical observations. Integrating Eq. (5) by parts and putting the result in iterative form yields

$$N_j - N_j^k = -\int_0^{y_t} (\tau_j^{k+1} - \tau_j^k)(\partial B_j/\partial y)\, dy \tag{7}$$

where N_j is the actual radiance for channel j and the superscripts k and $k+1$ refer to successive approximations to the quantities associated with them. Using the linear Taylor approximation, the transmittance change in Eq. (7) can be expressed as a function of the change in the optical depth $U_1(y)$ of the gas to be monitored to give

$$N_j - N_j^k = \int_0^{y_t} (U_1^{k+1} - U_1^k)(e^y/\omega_1^k)(\partial\tau_j^k/\partial y)(\partial B_j/\partial y)\, dy \tag{8}$$

where $U_1^k(y)$ is related to $\omega_1^k(y)$ by

$$U_1^k(y) = \int_y^{y_t} \omega_1^k e^{-y}\, dy$$

With the assumption[1] that the ratio $U_1^{k+1}(y)/U_1^k(y)$ is independent of y over the atmospheric layer sensed by channel j, Eq. (8) yields the $k+1$ estimate of ω_1 due to channel j as

$$\omega_{1,j}^{k+1}(y) = \left[1 + \frac{N_j - N_j^k}{S_j^k}\right]\omega_1^k(y) \tag{9}$$

where

$$S_j^k = \int_0^{y_t} (U_1^k e^y/\omega_1^k)(\partial B_j/\partial y)(\partial\tau_j^k/\partial y)\, dy \tag{10}$$

and where the relation $\omega_1^k = (-e^y)(\partial U_1^k/\partial y)$ has been used. Following Smith,[1] the best approximation to ω_1 is given by the weighted average of the j independent estimates as

$$\omega_1^{k+1}(y) = \left[\sum_j W_j^{k+1}\omega_{1,j}^{k+1}\right] \Big/ \sum_j W_j^{k+1} \tag{11}$$

where

$$W_j^{k+1}(y) = (\partial B_j/\partial y)(\partial\tau_j^k/\partial y) \tag{12}$$

The iterative procedure is terminated when the difference between N_j^k and N_j, averaged over all channels in an rms sense, either

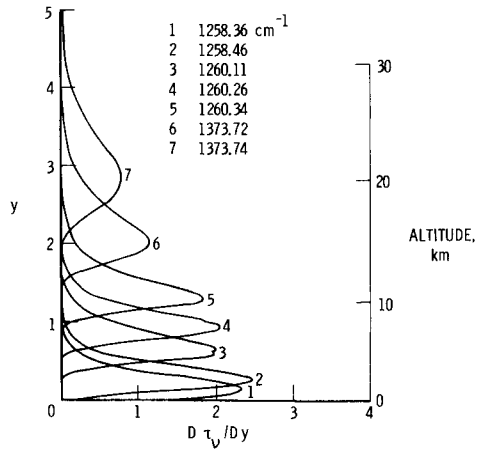

Fig. 2 Calculated weighting functions for H_2O vapor detection.

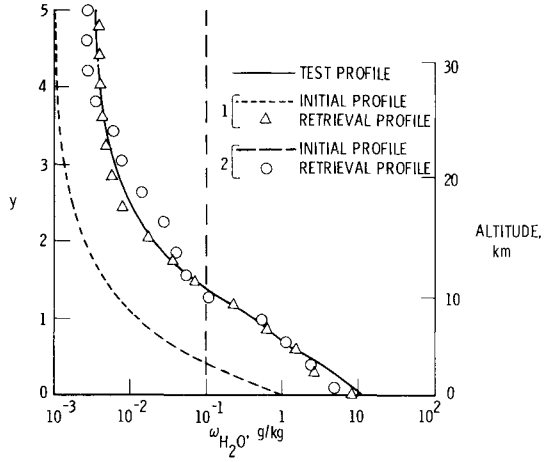

Fig. 4 Effect of initial-guess profile on ω_{H_2O} profile retrievals.

becomes less than a convergence criterion or converges to an asymptotic value.

Several assumptions, such as replacing $B(v, y)$ by $B_j(y)$ in obtaining Eq. (5) and removing the ratio $U_1^{k+1}(y)/U_1^k(y)$ from inside the integral over y in obtaining Eq. (9), have been made in deriving the retrieval procedure used in this work. These types of assumptions are made in the literature,[1,14] and one proof of their acceptability lies in the ability to obtain accurate profile retrievals with this procedure.

Calculations

In order to demonstrate the potential of a heterodyne radiometer with a tunable laser LO, numerical examples have been generated for application of such a device to remote sensing of vertical profiles of H_2O vapor and CH_4 up to 30 km altitude using the 7 to 8 μm spectral region. With lower spectral resolution (>2 cm^{-1}) devices, this spectral region has been thought to be of little use for measuring H_2O vapor or CH_4 due to interference between them.[14] Analysis of calculated high resolution atmospheric transmittances has been made to select narrow spectral channels for this work. Channels have been analyzed for maximum altitude coverage and minimum interference between H_2O vapor and CH_4. Seven H_2O vapor channels and six CH_4 channels have been selected. Interference from CH_4 is negligible for the H_2O channels, but H_2O vapor interference has to be considered for the CH_4 channels. Figures 2 and 3 show the calculated weighting functions for the H_2O and CH_4 channels, respectively, along with the center wave number $\bar{\nu}_j$ for each channel. For H_2O vapor, channels 1–5 are of the Case I type, while channels 6 and 7 are of Case II type. All six CH_4 channels are Case II channels. Since the radiance in each channel comes predominantly from the altitude range where $\partial\tau_j/\partial y$ is maximum, Figs. 2 and 3 indicate that these channels should provide good altitude coverage and discrimination for the 0 to 30 km altitude range.

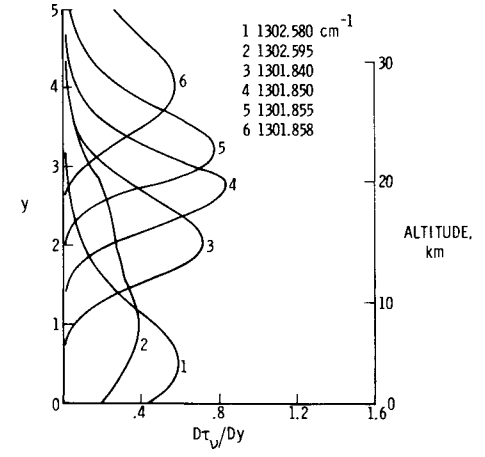

Fig. 3 Calculated weighting functions for CH_4 detection.

For all of the calculations presented here, a 45°N July U.S. standard atmosphere model has been used to provide the temperature profile up to 70 km altitude and a test H_2O vapor profile ω_{H_2O} up to 10 km altitude. Above 10 km, ω_{H_2O} has been assumed to decrease proportional to $e^{(p/p_0)}$ to a value of 3.1×10^{-3} g/kg. For CH_4 a test profile of 7.7×10^{-4} g/kg (1.4 ppm by volume) has been assumed up to 20 km altitude with an exponential decrease with altitude above 20 km. Transmittances have been calculated using a standard line-by-line absorption calculation with a Voigt line shape near line center and a Lorentz shape in the wings. Absorption line wing effects have been considered within 25 cm^{-1} of line centers for H_2O vapor and within 15 cm^{-1} of line centers for CH_4. Published absorption line parameters have been used for H_2O vapor[15] and CH_4,[16] and pressure and temperature effects on linewidths and line strengths have been included. The radiating-absorbing portion of the atmosphere has been assumed to lie between 0 and 70 km altitude, and this region has been broken up into 399 layers of equal Δy. Integrations over y which are required in the calculations of radiances and vertical transmittances and in the iterative retrieval scheme have been performed using a two-point numerical integration across each layer. Frequency integrations have been performed using three-point Legendre-Gauss quadrature.

Synthetic thermal radiances have been calculated for the H_2O vapor and CH_4 channels using Eq. (5), the assumed temperature profile, and the test H_2O and CH_4 profiles. The iterative procedure of Eqs. (9) and (11) has been used with these two sets of radiances to invert Eq. (5) and retrieve mass fraction profiles ω_i for H_2O vapor and CH_4. A series of retrieval calculations have been made for each gas to evaluate the procedure and the effects of various error sources by comparing the retrieval profiles with the test profiles used to calculate the channel radiances.

Results and Discussion

To initiate the iterative retrieval scheme, it is necessary to specify an initial guess or zero-order approximation for the ω_i profile of the gas being monitored. Figure 4 shows that, as would be hoped, the H_2O vapor retrieval profile does not depend significantly on the initial guess profile. Two totally dissimilar guess profiles, given by

$$\omega_{H_2O}{}^o = 10^{-3} \times e^{(6.908 p/p_0)} \text{g/kg} \qquad (13)$$

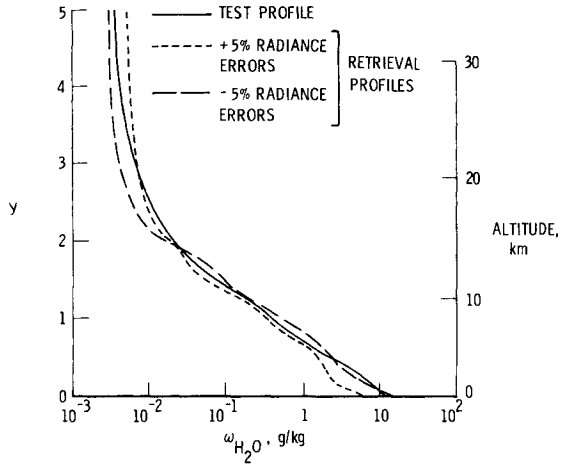

Fig. 5 Effect of radiance detection errors on ω_{H_2O} profile retrievals.

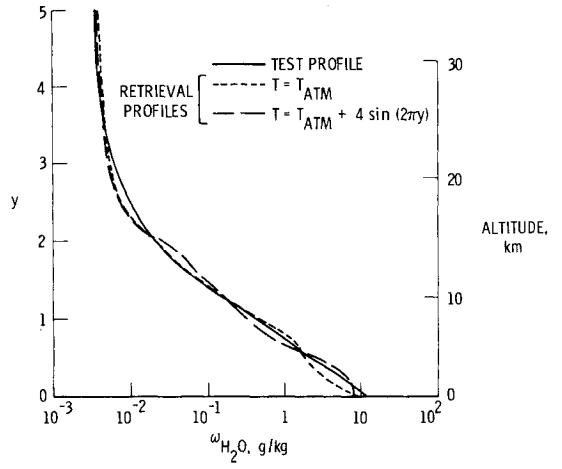

Fig. 6 Effect of a distributed temperature profile error on ω_{H_2O} profile retrievals.

and

$$\omega_{H_2O}{}^{o} = 10^{-1}\,\text{g/kg} \tag{14}$$

are shown, and the resulting retrieval profiles can be seen to compare favorably with each other and with the test profile. In both cases the shape and magnitude of the test profile are retrieved accurately over the entire altitude range considered. Results do indicate that an initial guess profile which is smaller than the actual profile gives slightly better retrievals, and thus the guess profile given by Eq. (13) is used for the subsequent ω_{H_2O} retrievals reported here.

Figure 5 shows that accurate retrievals of ω_{H_2O} can be made with radiance detection errors of up to 5%, corresponding to signal-to-noise ratios of 20. The retrievals shown here were made by perturbing the calculated radiance for each channel by $+5\%$ in one case and -5% in the second case and using these perturbed radiances in the retrieval procedure. Received signal calculations for the channels of Fig. 2 indicate that, from Eq. (1), signal-to-noise ratios of 20 or greater can be obtained with post-detection integration times of less than 7 sec for channels 1–5. Channels 6 and 7 would require 81 and 52 sec, respectively.

Figure 6 shows that a distributed temperature profile error of 4°K in magnitude has little effect on the average accuracy of ω_{H_2O} retrievals. A sinusoidal temperature error with an amplitude of 4°K and a period of $y = 1$ ($\simeq 7$ km) was imposed on the standard atmosphere profile. Figure 6 shows that the retrieval using this temperature profile and the retrieval using the standard atmosphere temperature profile compare equally well with the test ω_{H_2O} profile. A direct temperature bias error affects the retrieval profile in a different manner. Retrieval calculations were made using temperature profiles perturbed at all levels by $+2$°K in one case and -2°K in another case. The effects of this type of temperature error are practically identical to the effects of the $\pm 5\%$ radiance errors shown in Fig. 5.

Figure 7 illustrates that the effect of ground temperature variations upon the ω_{H_2O} retrievals is limited to the 2 to 3 km region above the ground. The radiances for the H_2O vapor channels were adjusted by changing $B_j(0)$ in Eq. (5) to account for ground temperature variations of ± 11°K from the standard atmosphere $y = 0$ temperature. Retrieval calculations were made using the two sets of adjusted radiances and the normal radiance set, and Fig. 7 shows that above 2.5 km altitude, the three retrievals are practically identical. In the retrievals, the standard temperature profile was used, with the effects of ground temperature variations arising only in the simulated channel radiances.

Retrieval calculations have also been performed for CH_4 using the radiances calculated for the six channels of Fig. 3. As mentioned previously, H_2O vapor contributes to the radiances and transmittances for these CH_4 channels and must be included in the calculations. It has been determined, however, that retrieval ω_{H_2O} profiles such as those shown in previous figures are sufficiently accurate to be used to calculate the interference effects of H_2O vapor. In an operational system, the ω_{H_2O} profile could be determined using the channels of Fig. 2 and then be used in determining the CH_4 profile.

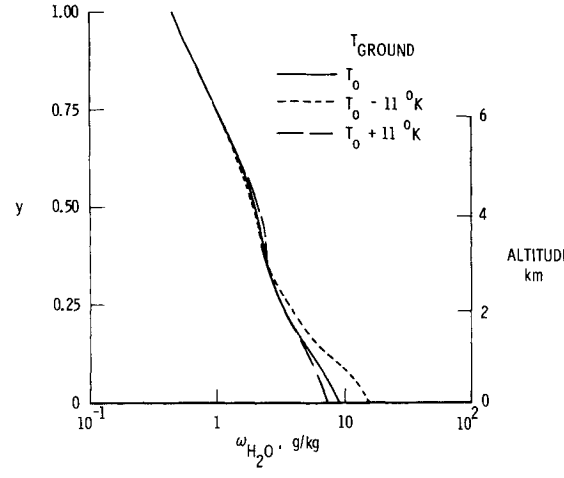

Fig. 7 Effect of ground temperature errors on ω_{H_2O} profile retrievals.

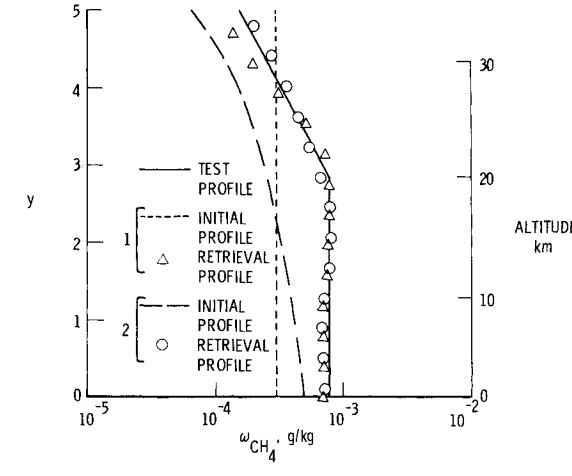

Fig. 8 Effect of initial-guess profile on ω_{CH_4} profile retrievals.

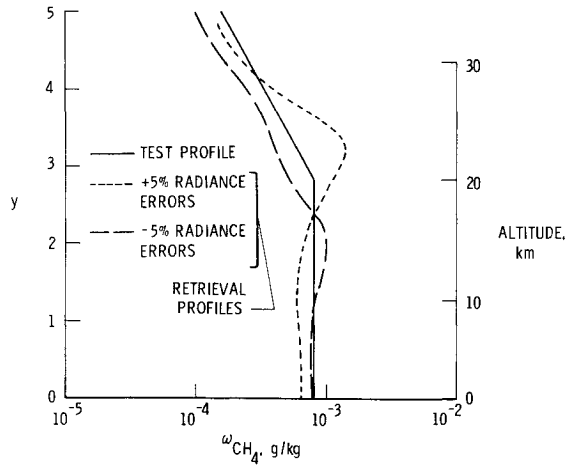

Fig. 9 Effect of radiance detection errors on ω_{CH_4} profile retrievals.

Figure 8 demonstrates that the ω_{CH_4} retrievals are not strongly dependent on the initial guess profile used to start the iterative retrieval procedure. Two initial guess profiles, given by

$$\omega_{CH_4}{}^{o} = \begin{cases} 10^{-4} \times (5-0.875y)\ \text{g/kg}, & y \leq 5 \\ 9.276 \times 10^{-3} \times e^{-y}\ \text{g/kg}, & y > 5 \end{cases} \quad (15)$$

and

$$\omega_{CH_4}{}^{o} = 3 \times 10^{-4}\ \text{g/kg} \quad (16)$$

are shown, and the resulting retrieval profiles are compared to the test CH_4 profile. Again, the initial guess profile which is smaller at all levels than the test profile gives slightly better retrievals, and thus the profile given by Eq. (15) is used as the initial guess in subsequent CH_4 retrieval calculations.

In Fig. 9 the effects of $\pm 5\%$ radiance detection errors on the ω_{CH_4} retrieval calculations are shown. Two retrievals were made using radiances adjusted by $\pm 5\%$ from the values calculated using Eq. (5). Figure 9 compares these two retrieval profiles with the test CH_4 profile and, in both cases, the retrievals compare well with the test profile except in the region around 20 km. The substantial error in this region is probably due to the combination of a sudden change in the test profile shape with the nearly isothermal atmosphere around 20 km. Calculations indicate that signal-to-noise ratios of 20 (corresponding to 5% detection error) could be obtained for the six CH_4 channels with postdetection integration times ranging from 1.2 sec for channel 1 to 26 sec for channel 4.

Summary and Conclusions

A detailed computer analysis has been presented for a high spectral resolution (10^8 Hz) tunable laser heterodyne radiometer capable of scanning individual atmospheric emission lines from satellite altitudes. The advantages of a tunable laser local oscillator have been indicated along with the feasibility of diode lasers for such use. Numerical retrievals of the vertical distribution profiles of H_2O vapor and CH_4 from radiances simulated for 10^8 Hz channels in the 7 to 8 μm spectral region have demonstrated the potential of such a system for remotely determining atmospheric gas profiles. The numerical examples have demonstrated that with the spectral resolution available in a heterodyne system it should be possible to monitor gases such as H_2O vapor and CH_4 in spectral regions which under lower spectral resolution have prohibitive interference between overlapping gases. Sensing channels can be selected with flexibility to provide minimum interferences and maximum altitude coverage. In the examples presented here, interference from CH_4 was eliminated in the channel selection for H_2O vapor. H_2O vapor interference remained for the CH_4 channels, but its effect was minimized. Good altitude coverage up to 30 km was demonstrated in both cases.

An analysis of potential error sources has indicated that radiance detection error of up to 5% (signal-to-noise of 20) and temperature bias errors of up to 2°K are allowable without serious degradation of the results. The required signal-to-noise level of 20 has been calculated to be achievable with reasonable postdetection integration times for all channels except the two high altitude H_2O channels which, for the conditions used in this work, would require 81 sec and 52 sec, respectively. Improvements in these two integration times could be made by increasing the spectral width of these two channels and adjusting the channel center $\bar{\nu}_j$ closer to the emission line center.

The calculations in this work used a model atmosphere typical of midlatitude summer conditions and assumed scattering effects to be negligible. Having demonstrated the potential of the heterodyne radiometer with these calculations, work is presently under way to include effects of real atmospheres and extreme atmospheric conditions. Calculations are also being performed to simulate measurements of other gases such as N_2O, O_3, SO_2, NH_3, and C_2H_4. In addition, experimental work with tunable diode lasers is being performed at Langley Research Center with one goal being the use of these lasers in a heterodyne radiometer.

References

[1] Smith, W. L., "Iterative Solution of the Radiative Transfer Equation for the Temperature and Absorbing Gas Profile of an Atmosphere," *Applied Optics*, Vol. 9, No. 9, Sept. 1970, pp. 1993–1999.

[2] Chahine, M. T., "A General Relaxation Method for Inverse Solution of the Full Radiative Transfer Equation," *Journal of the Atmospheric Sciences*, Vol. 29, May 1972, pp. 741–747.

[3] Kaplan, L. D., "Inference of Atmospheric Structure from Remote Radiation Measurements," *Journal of the Optical Society of America*, Vol. 49, No. 10, Oct. 1959, pp. 1004–1007.

[4] Smith, W. L. and Howell, H. B., "Vertical Distributions of Atmospheric Water Vapor from Satellite Infrared Spectrometer Measurements," *Journal of Applied Meteorology*, Vol. 10, Oct. 1971, pp. 1026–1034.

[5] Smith, W. L., Woolf, H. M., and Fleming, H. E., "Retrieval of Atmospheric Temperature Profiles from Satellite Measurements for Dynamical Forecasting," *Journal of Applied Meteorology*, Vol. 11, Feb. 1972, pp. 113–122.

[6] Houghton, J. T. and Smith, S. D., "Remote Sounding of Atmospheric Temperature from Satellites," *Proceedings of the Royal Society of London*, Vol. A320, 1970, pp. 23–33.

[7] Taylor, F. W., Houghton, J. T., Peskett, G. D., Rodgers, C. D., and Williamson, E. J., "Radiometer for Remote Sounding of the Upper Atmosphere," *Applied Optics*, Vol. 11, No. 1, Jan. 1972, pp. 135–141.

[8] Teich, M. C., "Infrared Heterodyne Detection," *Proceedings of the IEEE*, Vol. 56, No. 1, Jan. 1968, pp. 37–46.

[9] Peyton, B. J., DiNardo, A., Kanischak, G., Lange, R., and Arams, F. R., "High-Sensitivity Receiver for CO_2 Laser Applications," Paper 16.6 presented at the Conference on Laser Engineering and Applications, June 1971, Optical Society of America, Washington, D.C.

[10] Hinkley, E. D. and Kingston, R. H., "Remote Heterodyne Detection of Gaseous Pollutants with Tunable Lasers," AIAA Paper 71-1079, Palo Alto, Calif., 1971.

[11] McElroy, J. H., "Infrared Heterodyne Solar Radiometry," *Applied Optics*, Vol. 11, No. 7, July 1972, pp. 1619–1622.

[12] Menzies, R. T., "Remote Detection of SO_2 and CO_2 with a Heterodyne Radiometer," *Applied Physics Letters*, Vol. 22, No. 11, June 1973, pp. 592–593.

[13] Allario, F., Seals, R. K., Jr., Brockman, P., and Hess, R. V., "Tunable Semiconductor Lasers and Their Application to Environmental Sensing," *Proceedings of the 10th Anniversary Meeting of the Society of Engineering Science*, Nov. 1973.

[14] Fritz, S., Wark, D. Q., Fleming, H. E., Smith, W. L., Jacobowitz, H., Hilleary, D. T., and Alishouse, J. C., "Temperature Sounding from Satellites," TR NESS 59, July 1972, National Oceanic and Atmospheric Administration, Washington, D.C.

[15] Benedict, W. S. and Calfee, R. F., "Line Parameters for the 1.9 and 6.3 Micron Water Vapor Lines," Professional Paper 2, June 1967, Environmental Science Services Administration, Washington, D.C.

[16] Kyle, T. G., "Line Parameters of the Infrared Methane Bands," AFCRL-68-0521, Oct. 1968, Air Force Cambridge Research Labs., Bedford, Mass.